

# Navigability of complex networks

Marián Boguñá,<sup>1</sup> Dmitri Krioukov,<sup>2</sup> and kc claffy<sup>2</sup>

<sup>1</sup>*Departament de Física Fonamental, Universitat de Barcelona, Martí i Franquès 1, 08028 Barcelona, Spain*

<sup>2</sup>*Cooperative Association for Internet Data Analysis (CAIDA), University of California, San Diego (UCSD), 9500 Gilman Drive, La Jolla, CA 92093, USA*

Targeted or quasi-targeted propagation of information is a fundamental process running in complex networked systems. Optimal communication in a network is easy to achieve if all its nodes have a full view of the global topological structure of the network. However many complex networks manifest communication efficiency without nodes having a full view of the network, and yet there is no generally applicable explanation of what mechanisms may render efficient such communication in the dark. In this work we model this communication as an oblivious routing process greedily operating on top of a network and making its decisions based only on distances within a hidden metric space lying underneath. Abstracting intrinsic similarities among networked elements, this hidden metric space is not easily reconstructible from the visible network topology. Yet we find that the structure of complex networks observed in reality, characterized by strong clustering and specific values of exponents of power-law degree distributions, maximizes their navigability, i.e., the efficiency of the greedy path-finding strategy in this hidden framework. We explain this observation by showing that more navigable networks have more prominent hierarchical structures which are congruent with the optimal layout of routing paths through a network. This finding has potentially profound implications for constructing efficient routing and searching strategies in communication and social networks, such as the Internet, Web, etc., and merits further research that would explain whether navigability of complex networks does indeed follow naturally from specifics of their evolution.

## I. INTRODUCTION

Complex networks permeate a variety of aspects of daily human life, remarkable and in some cases disconcerting given limited understanding of them [1]. For the last few years, complex network science research has focused heavily on understanding the topological structure of complex networks. However, this structure cannot be fully understood in disentanglement from the processes running *on* complex networks that shape or use it [1]. Many such processes are forms of information propagation. Data communication networks (e.g., the Internet), social networks, biological networks (e.g., signaling pathways, neural networks, etc.) typify networks where efficiency of information exchange plays a definitive role. Nodes in these networks manage somehow to find intended communication targets even though they do not possess any global view of the network.

The main purpose of this paper is to demonstrate that the observed peculiarities of complex network topologies are as needed for efficient communications in the dark, i.e., when nodes do not know the global topology of their own network. Besides its fundamental significance, one of the potential practical applications, and motivations, for this work is routing in the Internet. Scalability of the existing Internet routing architecture is approaching its fundamental limits [2], primarily due to the requirement that all nodes must have a coherent full view of the network topology [3]. Therefore an outstanding challenge is to design routing architectures that would not require such precise global knowledge.

The first popular demonstration that global knowledge is not required for efficient global communication in com-

plex networks was from Milgram [4]. His experiments indicated that social acquaintance networks are navigable small worlds: short paths prevail and nodes can find them. Nodes in these experiments were humans asked to forward a letter to one of their friends that, in the current node's opinion, would maximize the probability that the letter moves closer to its destination. Nodes thus possess only local topological information. They are aware only of: 1) their neighbors in the global acquaintance network; and 2) some attributes of those neighbors, such as place of living, occupation, etc. Having only this limited information, nodes can still propagate information to a target efficiently. To quantify, the percentage of successfully delivered messages in the original experiments was around 30% [4], while their subsequent simple modifications improved it up to 90% [5].

Milgram's surprising findings have seen significant research interest recently [6], including the notable Kleinberg model [7]. In this model, attributes of nodes are their coordinates in a two-dimensional lattice. Knowing their own coordinates, coordinates of their neighbors, and the coordinates of a destination, nodes can quickly compute distances in the lattice and select as the next hop the neighbor closest to the destination in the lattice. Following [7], we will refer to this opportunistic forwarding process as *greedy routing*.

Unfortunately, besides few notable exceptions [8, 9, 10], neither the Kleinberg model nor the substantial amount of subsequent literature (see review [6]) examine whether the greedy routing efficiency observed in Milgram's experiments is related to peculiarities of complex network topologies. Most complex networks, including social networks in Milgram's experiments, are characterized by strong clustering, i.e., high concentration of

triangular subgraphs, and by heterogenous degree distributions that are scale-free, e.g., follow power laws. The Kleinberg model and its generalizations do not naturally produce scale-free graphs. Most such models generate graphs with all nodes of the same degree, which induces quite different topological properties from those of complex networks. Since routing efficiency depends crucially on the network topology [3], a tempting hypothesis is that the efficiency of greedy routing on complex networks is related to their topological structure.

In this paper we show that the scale-free structure of complex network topologies and the efficiency of greedy routing on them cannot be decoupled. We first extend the Kleinberg formalism and let all nodes of a complex network reside in a hidden metric space, meaning that for every pair of nodes we define a hidden distance between them that initially is not directly related to the structure of the visible network. These settings allow us to use the powerful hidden-variable formalism [11] to introduce a model of scale-free networks with peculiar self-similar hierarchical structure that is tightly coupled with an underlying hidden distance oracle. We use this model to show that strong clustering and exponents of power-law degree distributions, empirically observed in many real complex networks, maximizes their navigability measured as the efficiency of greedy routing on them. We explain all our findings with in-depth analytic results confirmed by extensive simulations. We demonstrate that greedy routing increases its efficiency by implicitly utilizing the peculiar hierarchical organization of networks in our model, a consequence of an intricate interplay between visible and hidden characteristics of nodes, links, and paths, i.e., between their topological and geometric attributes.

## II. SCALE-FREE NETWORKS OVER HIDDEN METRIC SPACES

### A. Random networks with hidden variables

Random networks with hidden variables [11] offer a simple yet powerful formalism for analysis of complex networks. It tremendously simplifies, in some cases even makes tractable, a number of involved analytic calculations concerning complex network topologies. In this formalism, each node is assigned a hidden random variable  $h$  distributed according to some probability distribution  $\rho(h)$ , while links between pairs of nodes with hidden variables  $h$  and  $h'$  are established with some probability  $r(h, h')$ . A conceptual motivation for this approach is that in many complex systems, probabilities of connections between elements depend on some intrinsic properties—hidden variables—of these elements. In a real network, hidden variables can correspond to any kind of node attributes relevant for network formation. They can be, for example, country gross domestic products explaining the topological properties of the world trade web [12], or free energies in protein interaction

networks [13]. For the purposes of this paper, hidden variables can be hidden distances between nodes.

### B. Hidden distances as hidden variables

The most general way to introduce hidden distances is to assume that all nodes reside in a hidden metric space  $\mathcal{H}$ , i.e., each pair of nodes  $v, u \in \mathcal{H}$  are at a certain hidden distance  $h_{vu}$  from each other, and observable random graphs  $G$  are formed by creating links between  $v$  and  $u$  with probability  $r(h_{vu})$ . All nodes have thus two “lives”—in the hidden space  $\mathcal{H}$  and in the observable graph  $G$ . If  $r$  is a decreasing function, then the strong clustering ubiquitously observed in complex networks modeled by graphs  $G$  finds a natural explanation via the triangle inequality in  $\mathcal{H}$ : if distances  $h_{vu}$  and  $h_{ut}$  are small, then  $h_{tv}$  is also small because of the triangle inequality, and all probabilities  $r(h_{vu})$ ,  $r(h_{ut})$ , and  $r(h_{tv})$  are high. In other words, all three links of triangle  $vut$  in  $G$  exist with high probability, thus increasing clustering.

A generic metric space  $\mathcal{H}$  requires  $O(N \log N)$  bits of information at each node in order to store distances to all other  $N$  nodes in  $\mathcal{H}$ . The same amount of information is required to store shortest-path routing tables for a generic  $N$ -sized graph  $G$ . Therefore the global knowledge of  $G$  is equivalent, in terms of required information, to the global knowledge of  $\mathcal{H}$ , if  $\mathcal{H}$  is generic [14]. However, if  $\mathcal{H}$  is embeddable in a  $D$ -dimensional normed space or Riemannian manifold, then the amount of information required to compute distances in  $\mathcal{H}$  reduces to  $O(D \log N)$  per node [14]. Dimension  $D$  roughly models the number of different node attributes in Milgram’s experiments [7], and this number was small [4]. This observation motivates us to study greedy routing in scale-free graphs residing in low-dimensional normed spaces or Riemannian manifolds. The simplest such space is the one-dimensional sphere  $\mathbb{S}^1$ .

### C. A model with $\mathbb{S}^1$ as a hidden metric space

In the  $\mathbb{S}^1$  model we place all nodes on a circle by assigning them a random variable  $\theta$ , i.e., their polar angle, distributed uniformly in  $[0, 2\pi)$ . The circle radius  $R$  grows linearly with the total number of nodes  $N$ ,

$$2\pi R = N, \quad (1)$$

in order to keep the average density of nodes on the circle fixed to 1. Since the distribution of nodes on  $\mathbb{S}^1$  is homogeneous, no connection probability function  $r$  can give rise to heterogenous scale-free degree distributions in graphs  $G$ . To construct scale-free graphs, we have to assign an additional hidden random variable  $\omega$  to all nodes. There are no correlations between  $\theta$  and  $\omega$ , meaning that the joint distribution

$$\rho(\theta, \omega) = \rho(\theta)\rho(\omega), \quad (2)$$

where  $\rho(\theta) = 1/(2\pi)$  and  $\rho(\omega)$  is to control the degree distribution in  $G$ .

The simplest way to instrument such control is to ensure that the average degree  $\bar{k}(\omega)$  of nodes with hidden variable  $\omega$  is proportional to  $\omega$ . The first step to guarantee this condition is to let the connection probability between two nodes with hidden coordinates  $(\theta, \omega)$  and  $(\theta', \omega')$  be of the form

$$r(\theta, \omega; \theta', \omega') = r \left( \frac{d(\theta, \theta')}{d_c(\omega, \omega')} \right), \quad (3)$$

where

$$d(\theta, \theta') = R \min(|\theta - \theta'|, 2\pi - |\theta - \theta'|) \quad (4)$$

is the geodesic distance between the two nodes in  $\mathbb{S}^1$ , and  $d_c(\omega, \omega')$  is a *characteristic distance scale* between nodes with variables  $\omega$  and  $\omega'$ . Informally, since  $\omega$  is to be proportional to node degree, distance scale  $d_c(\omega, \omega')$  should be a symmetric increasing function of its arguments because we expect nodes with higher degrees to cover larger zones of  $\mathbb{S}^1$  with their connections. To formally determine  $d_c(\omega, \omega')$ , we note that if functions  $\rho$  and  $r$  are as in Eqs. (2-3),  $N$  is large, and  $\rho(\omega)$  decreases sufficiently fast, then the average degree of nodes with hidden coordinates  $(\theta, \omega)$ ,  $\bar{k}(\theta, \omega) = N \int r(\theta, \omega; \theta', \omega') \rho(\theta', \omega') d\theta' d\omega'$ , reduces to  $\bar{k}(\theta, \omega) = \bar{k}(\omega) \sim \int d_c(\omega, \omega') \rho(\omega') d\omega'$  after integrating over  $\theta'$  and omitting all constants. Choosing the characteristic distance scale as

$$d_c(\omega, \omega') = \kappa \omega \omega', \quad (5)$$

with appropriate constant  $\kappa > 0$ , we thus ensure that

$$\frac{\bar{k}(\omega)}{\langle k \rangle} = \frac{\omega}{\langle \omega \rangle}, \quad (6)$$

where  $\langle k \rangle$  and  $\langle \omega \rangle$  denote the average degree and average value of  $\omega$ .

Proportionality between  $\omega$  and  $\bar{k}(\omega)$  in Eq. (6) guarantees that the shape of the node degree distribution  $P(k)$  in  $G$  is approximately the same as the shape of  $\rho(\omega)$  in  $\mathcal{H}$ . Indeed, as shown in [11],

$$P(k) = \int e^{-\bar{k}(\omega)} \frac{\bar{k}^k(\omega)}{k!} \rho(\omega) d\omega. \quad (7)$$

Since the Poisson kernel in this integral is sharply peaked around  $k \approx \bar{k}(\omega)$ , Eq. (6) implies that the tail of  $P(k)$  behaves exactly as the tail of  $\rho(\omega)$ . We thus can generate graphs with any degree distribution by choosing an appropriate  $\rho(\omega)$ . In particular, to generate scale-free graphs we set

$$\rho(\omega) = (\gamma - 1) \omega^{-\gamma}, \quad \omega > 1, \quad \gamma > 2. \quad (8)$$

Substituting this expression in Eq. (7) yields the degree distribution

$$P(k) = \frac{(\gamma - 1)}{k!} \left( \frac{\gamma - 2}{\gamma - 1} \langle k \rangle \right)^{\gamma-1} \Gamma(k + 1 - \gamma, \frac{\gamma - 2}{\gamma - 1} \langle k \rangle), \quad (9)$$

where  $\Gamma$  is the incomplete gamma function. The asymptotic behavior of this degree distribution for large  $k$  is  $P(k) \sim k^{-\gamma}$ , i.e., the same as of  $\rho(\omega)$  from Eq. (8). In Appendix A we show the degree distributions of graphs generated in simulations implementing our model. The simulations match perfectly our analytic results in Eq. (9).

Before proceeding to specify an exact form of the connection probability  $r$  in the  $\mathbb{S}^1$  model, we pause to notice that we have not relied on any conditions specific to  $\mathbb{S}^1$  thus far. The only requirement we depend on to control the degree distribution in  $G$  is the linear dependency of  $\bar{k}(\omega)$  on  $\omega$  in Eq. (6), which relies only upon Eqs. (2-5). Nodes could be uniformly distributed, for example, on a  $D$ -dimensional sphere  $\mathbb{S}^D$ , but Eq. (6) would still hold if  $\rho$  and  $r$  factorized as in Eqs. (2) and (3), and if the characteristic distance scale were  $d_c(\omega, \omega') = (\kappa \omega \omega')^{1/D}$  instead of Eq. (5). In other words, we can fully control the degree distribution in observable graphs  $G$  regardless of the dimension of the hidden space  $\mathcal{H}$ . This observation is yet another justification to model  $\mathcal{H}$  the simplest way—by  $\mathbb{S}^1$ .

Going back to our  $\mathbb{S}^1$  model, we specify the connection probability  $r$  such that we can control clustering in generated graphs  $G$ . Specifically, we define  $r$ , compliant with Eqs. (3-5), as

$$r(\theta, \omega; \theta', \omega') = \left( 1 + \frac{d(\theta, \theta')}{\kappa \omega \omega'} \right)^{-\alpha}, \quad \alpha > 1, \quad (10)$$

where the value of constant  $\kappa = (\alpha - 1)\langle k \rangle / (2\langle \omega \rangle^2)$  follows from the normalization  $\langle k \rangle = N \int \rho(\theta, \omega) r(\theta, \omega; \theta', \omega') \rho(\theta', \omega') d\theta d\omega d\theta' d\omega'$  for large  $N$ . Parameter  $\alpha$  controls clustering because the larger  $\alpha$  is, the more preferred are short-distance connections, thus more triangles are formed. In Appendix B we analytically compute the clustering coefficient, i.e., mean clustering in graphs  $G$ . The qualitative outcome of this computation is that mean clustering vanishes when  $\alpha \rightarrow 1$  and converges to a constant value, dependent on  $\gamma$ , when  $\alpha \rightarrow \infty$ . Conditions  $\alpha > 1$  in Eq. (10) and  $\gamma > 2$  in Eq. 8 guarantee that modeled graphs  $G$  are sparse, i.e., they have finite average degree  $\langle k \rangle$  in the large-graph limit  $N \rightarrow \infty$ .

In summary, the model that we have constructed has several powerful features: (a) it produces random networks with nodes that reside in a hidden metric space; (b) we have complete control over degree distribution in these networks, thus we can generate scale-free networks with power-law degree distributions; (c) keeping the degree distribution fixed, we can also alter clustering in generated networks; and (d) as we show in Appendices C and D, the generated networks are self-similar small worlds. In the next section, we exploit properties (a-c) to study the performance of greedy routing in our model.

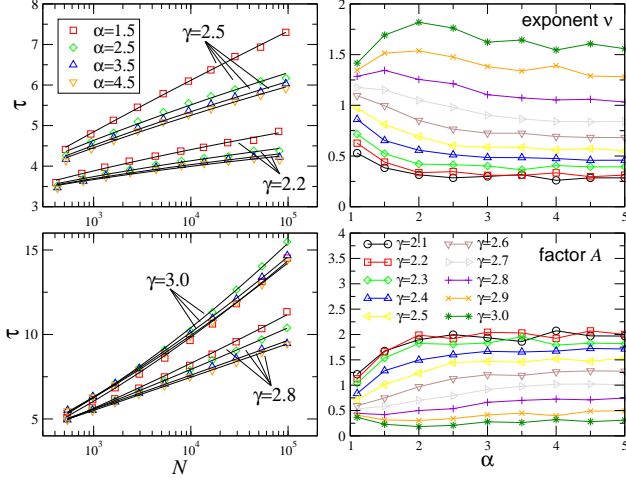


FIG. 1: **Average length  $\tau$  of greedy-routing paths.** The left two plots show  $\tau$  as a function of the network size  $N$  for different values of  $\gamma$  and  $\alpha$ . In all cases, the observed values of  $\tau$  are fit well by  $\tau(N) = A[\log N]^\nu$ . The right two plots show factors  $A$  and exponents  $\nu$  of these fits for all  $(\gamma, \alpha)$  pairs.

### III. PERFORMANCE OF GREEDY ROUTING IN THE MODEL

We first perform simulations to study two navigability characteristics of modeled scale-free (SF) networks: 1) the average hop length  $\tau$  of successful greedy-routing (GR) paths, i.e., the paths that reach a destination, and 2) the percentage  $p_s$  of successful paths.

Our model has three independent parameters: exponent  $\gamma$  of power-law degree distributions, clustering strength  $\alpha$ , and average degree  $\langle k \rangle$ . We fix the latter to 6, which is roughly equal to the average degree of some real networks of interest [15, 16], and vary  $\gamma \in [2.1, 3]$  and  $\alpha \in [1.1, 5]$ , covering their observed ranges in documented complex networks [17]. For each  $(\gamma, \alpha)$  pair, we produce graphs of different sizes  $N \in [10^3, 10^5]$  generating, for each  $(\gamma, \alpha, N)$ , a number of different graph instances—from 40 for large  $N$  to 4000 for small  $N$ . In each graph instance  $G$ , we randomly select  $10^6$  source-destination pairs  $(a, b)$  and execute the GR process for them starting at  $a$  and selecting, at each hop  $h$ , the next hop as the  $h$ 's neighbor in  $G$  closest to  $b$  in the hidden metric space  $\mathbb{S}^1$ . If for a given  $(a, b)$ , this process visits the same node twice, then the corresponding path leads to a loop and is unsuccessful. We then average the measured values of  $\tau$  and  $p_s$  across all pairs  $(a, b)$  and graphs  $G$  for the same  $(\gamma, \alpha, N)$ . We show the results in Figs. 1 and 2.

Both figures tell a similar story: small power-law exponents and strong clustering observed in many complex networks improve network navigability. Indeed, if we fix  $\gamma$  and  $N$ , then stronger clustering (higher  $\alpha$ ) generally corresponds to shorter paths (smaller  $\tau$ ) and larger proportions of successful paths  $p_s$ .

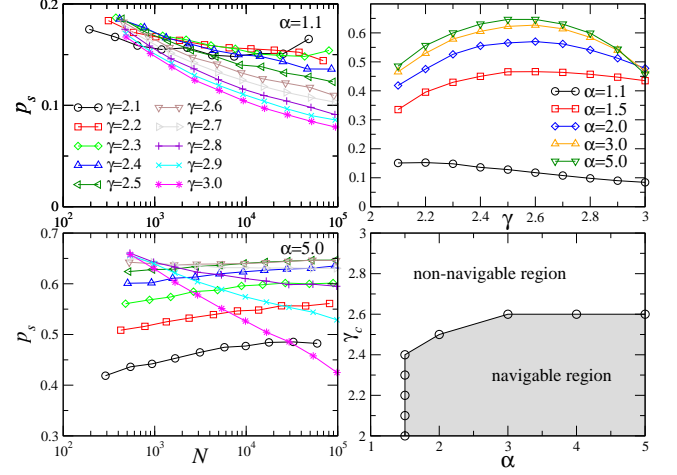


FIG. 2: **Success probability  $p_s$  of greedy routing.** The left plots show  $p_s$  as a function of network size  $N$  for different values of  $\gamma$  with weak (top) and strong (bottom) clustering. The top-right plot shows  $p_s$  as a function of  $\gamma$  for different clustering  $\alpha$  and  $N \approx 10^5$ . For each  $\alpha$ , there is a unique value of  $\gamma$ ,  $\gamma_c(\alpha)$ , which maximizes  $p_s(\gamma)$ . The bottom-right plot shows the curve  $\gamma_c(\alpha)$  separating the low- $\gamma$ , high- $\alpha$  navigable region in which greedy routing sustains in the large-graph limit ( $p_s(N)$  grows with  $N$ ) from the high- $\gamma$ , low- $\alpha$  non-navigable region where the efficiency of greedy routing degrades for large networks ( $p_s(N) \xrightarrow{N \rightarrow \infty} 0$ ).

We observe a less straightforward behavior with respect to  $\gamma$ . Paths are generally shorter for smaller  $\gamma$ . In all cases, we observe (Fig. 1) a polylogarithmic, i.e., small-world, growth of path lengths  $\tau(N)$  with the network size  $N$ . As  $\gamma$  decreases, there is an interesting transition from super- to sub-logarithmic growth of  $\tau(N)$  around  $\gamma = 2.6 \pm 0.1$ . However, although values of  $\gamma \rightarrow 2^+$  minimize path length  $\tau$ , larger  $\gamma$ -values increase the proportion of successful paths  $p_s$ . Indeed, the value of  $\gamma = 2.5 \pm 0.1$  maximizes  $p_s$ , as soon as clustering is above a certain threshold,  $\alpha \geq 1.5$ . Furthermore, if clustering is weak,  $p_s(N)$  decreases with  $N$  (Fig. 2 top-left), but with strong clustering,  $p_s(N)$  actually grows with  $N$  (Fig. 2 bottom-left) for values of  $\gamma$  up to  $2.5 \pm 0.1$ . If  $\gamma$  is above this critical value, then  $p_s(N)$  becomes a decreasing function again. These observations mean that for each  $\alpha$  there is a critical value of  $\gamma$  (Fig. 2 right) below (above) which growing networks remain (stop being) navigable as their size increases.

In summary, strong clustering improves both navigability metrics, and there is a delicate trade-off between values of  $\gamma$  close to 2 minimizing path lengths, and higher values, not exceeding  $\gamma \approx 2.6$ , maximizing the percentage of successful paths. We explain the observed phenomena in the following sections, but we note here that qualitatively, *this navigable parameter region contains a majority of complex networks observed in reality* [17].

#### IV. HIERARCHICAL ORGANIZATION OF MODELED NETWORKS

The routing process in our framework resembles guided searching for a specific object in a complex collection of objects. Perhaps the simplest and most general way to make a complex collection of heterogeneous objects searchable is to classify them in a hierarchical fashion. By “hierarchical,” we mean that the whole collection is split into categories (i.e., sets), sub-categories, sub-sub-categories, and so on. Relationships between categories form (almost) a tree, whose leaves are individual objects in the collection [18, 19]. Finding an object reduces to the simpler task of navigating this tree. We thus want to check first if the SF networks in our model possess any kind of hierarchical organization, and if so, whether navigability-related properties of this hierarchy vary with the model parameters.

$k$ -core decomposition [21, 22] is possibly the most suitable generic tool to expose hierarchy within our modeled networks. The  $k$ -core of a network is its maximal subgraph such that all the nodes in the subgraph have  $k$  or more connections to other nodes in the subgraph. A node’s coreness is the maximum  $k$  such that the  $k$ -core contains the node but the  $k+1$ -core does not. The  $k$ -core structure of a network is a form of hierarchy since a  $k+1$ -core is a subset of a  $k$ -core. One can estimate the quality of this hierarchy using properties of the  $k$ -core spectrum, i.e., the distribution of  $k$ -core sizes. If the maximum node coreness is large and if there is a rich collection of comparably-sized  $k$ -cores with a wide spectrum of  $k$ ’s, then this hierarchy is deep and well-developed, making it potentially more navigable. It is poor, non-navigable otherwise.

In Fig. 3 we feed real and modeled networks to the Large Network visualization tool (LaNet-vi) [20] which utilizes node coreness to visualize the network. Fig. 3 shows that networks with stronger clustering and smaller exponents of degree distribution possess stronger  $k$ -core hierarchies. These hierarchies are directly related to how networks are constructed in our model, since nodes with higher  $\omega$  and, consequently, higher degrees have generally higher coreness, as we can partially see in Fig. 3 and elaborate on in Appendix E. The remaining salient question is if the GR process can utilize these hierarchies for its benefit.

#### V. NAVIGABILITY THROUGH THE NETWORK HIERARCHY

##### A. Analytic results

To investigate whether GR exploits existing hierarchical organization of our modeled networks, we examine the structure of paths that GR produces. We start with the GR propagator that describes the hop-by-hop properties of GR-produced paths. Specifically, this one-hop propa-

gator  $G(\theta', \omega' | \theta, \omega; \theta_t)$  is the probability that a  $(\theta', \omega')$ -labeled node, i.e., a node whose hidden variables are  $(\theta', \omega')$ , is the next hop after a  $(\theta, \omega)$ -labeled node along a GR path toward destination  $t$  located at  $\theta_t$ . We use the hidden variable formalism to analytically calculate this propagator in Appendix F. The result is

$$G(\theta', \omega' | \theta, \omega; \theta_t) = \frac{N \rho(\theta', \omega') r(\theta', \omega'; \theta, \omega)}{1 - e^{-\bar{k}(\theta, \omega | \theta', \theta_t)}} e^{-\bar{k}(\theta, \omega | \theta', \theta_t)}, \quad (11)$$

where  $\bar{k}(\theta, \omega | \theta', \theta_t)$  is the average number of links between a  $(\theta, \omega)$ -labeled node and nodes lying at distance from  $t$  smaller than  $d(\theta', \theta_t)$ ,

$$\bar{k}(\theta, \omega | \theta', \theta_t) = N \int_{\mathcal{A}} d\theta'' \int d\omega'' \rho(\theta'', \omega'') r(\theta'', \omega''; \theta, \omega), \quad (12)$$

where  $\text{arc } \mathcal{A} = \{ \theta'' \mid d(\theta'', \theta_t) < d(\theta', \theta_t) \}$ .

A slightly more balanced form of the propagator in (11) is the probability  $G(d', \omega' | d, \omega)$  that an  $\omega'$ -labeled node located at hidden distance  $d'$  from the destination is the next hop after an  $\omega$ -labeled node at hidden distance  $d$  from the destination. Since  $\rho(\theta)$  is uniform and  $\mathbb{S}^1$  is isotropic, we can write this propagator as

$$G(d', \omega' | d, \omega) = \int \delta(d(\theta', \theta_t) - d') G(\theta', \omega' | \theta, \omega; \theta_t) d\theta', \quad (13)$$

where  $\delta$  stands for the delta function and  $d = d(\theta, \theta_t)$ . Substitution of Eqs. (2-5,8,10) into (11-13) yields a rather long closed-form expression for propagator  $G(d', \omega' | d, \omega)$  which we give in Appendix F. Here we are more interested in statistics defined by this propagator that elucidate the GR path structure.

Specifically, in Fig. 4 we show the probability  $P_{\text{back}}(\omega, d)$  that an  $\omega$ -labeled node at hidden distance  $d$  from a destination has no neighbor closer to the destination than itself,

$$P_{\text{back}}(\omega, d) = \int_{d' \geq d} dd' \int d\omega' G(d', \omega' | d, \omega), \quad (14)$$

in which case a GR path goes back to the previous hop and consequently fails. Fig. 4 shows that  $P_{\text{back}}(\omega, d)$  is an exponentially decreasing function of  $\omega$ . For fixed  $\omega$  and  $d$ ,  $P_{\text{back}}(\omega, d)$  also decreases with  $\gamma$ . These two effects are related since the former implies that most paths are lost in the low- $\omega$  network periphery and this periphery is relatively larger for lower values of  $\gamma$ , cf. Appendix A.

In Fig. 5 we show the probability  $P_{\text{up}}(\omega, d)$  that the next hop after an  $\omega$ -labeled node located at hidden distance  $d$  from a destination has value  $\omega'$  larger than  $\omega$ , and is closer to the destination,

$$P_{\text{up}}(\omega, d) = \int_{\omega' \geq \omega} d\omega' \int_{d' < d} dd' G(d', \omega' | d, \omega), \quad (15)$$

in which case the path goes “up” in the hierarchy toward the high- $\omega$  network core.



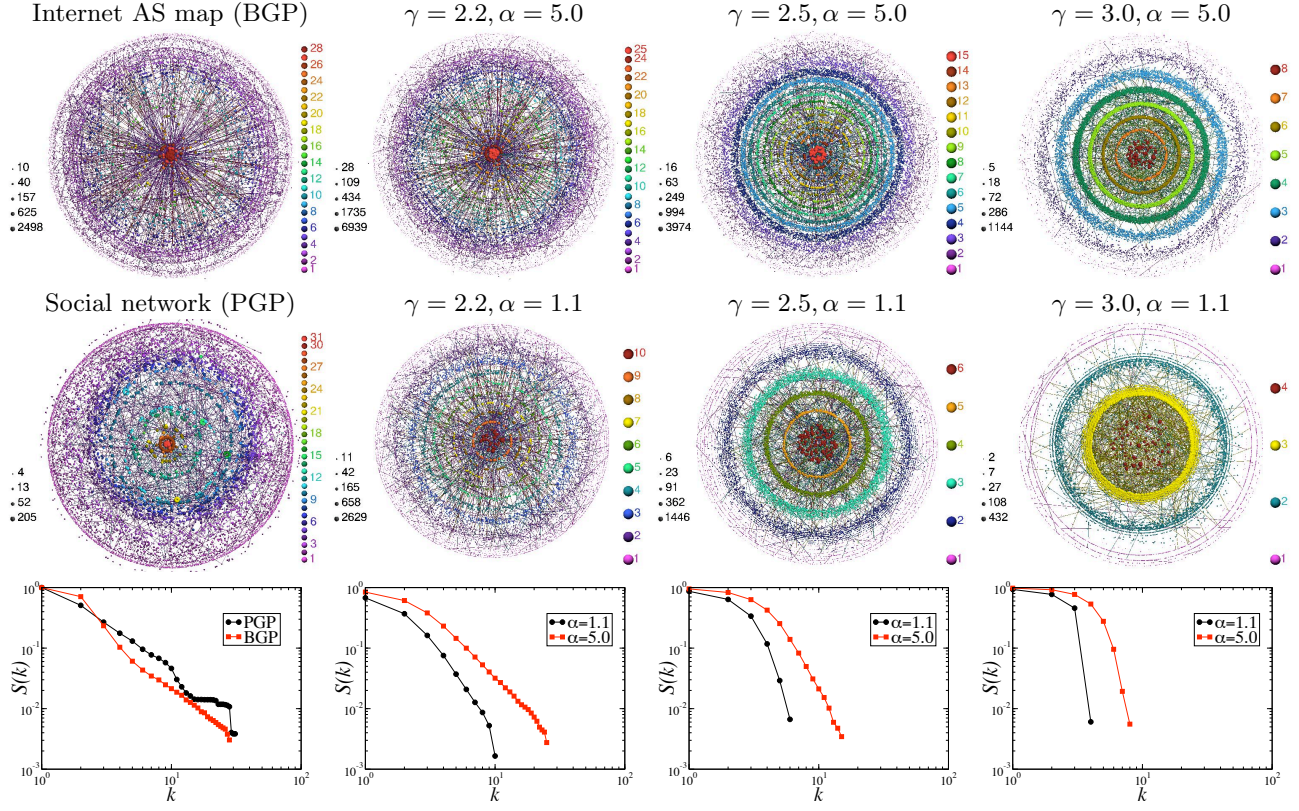


FIG. 3:  **$k$ -core decompositions of real and modeled networks.** The first two rows show LaNet-vi [20] network visualizations. All nodes are color-coded based on their coreness (right legends) and size-coded based on their degrees (left legends). Higher-coreness nodes are closer to circle centers. The third row shows the  $k$ -core spectrum, i.e., the distribution  $\mathcal{S}(k)$  of sizes of node sets with coreness  $k$ . The first column depicts two real networks: the AS-level Internet as seen by the Border Gateway Protocol (BGP) in [15] and the Pretty Good Privacy (PGP) social network from [16]. The rest of the columns show modeled networks for different values of power-law exponent  $\gamma$  in cases with weak ( $\alpha = 1.1$ ) and strong ( $\alpha = 5.0$ ) clustering. The network size  $N$  for all real and modeled cases is approximately  $10^4$ . Similarity between real networks and modeled networks with low  $\gamma$  and high  $\alpha$  is remarkable.

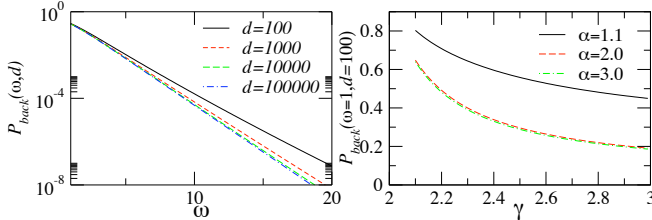


FIG. 4: **Probability  $P_{back}(\omega, d)$**  that an  $\omega$ -labeled node at distance  $d$  from a destination has no neighbor closer to the destination than itself. Parameters  $\gamma = 2.5$  and  $\alpha = 5.0$  in the left plot, while  $\omega = 1$  and  $d = 100$  on the right. Curves with other parameter values are qualitatively the same. The results are for the large-graph limit  $N \rightarrow \infty$ .

Fig. 5 confirms that the GR process does make use of hierarchical structure when present in the network, cf. Fig. 3. In the most navigable case with low degree-distribution exponent  $\gamma = 2.2$  and strong clustering  $\alpha = 5.0$ ,  $P_{up}(\omega, d)$  is large if  $\omega$  is small, and it quickly drops to zero if  $\omega$  becomes larger than a certain critical value

$\omega_c$ , which increases with distance  $d$ . This observation implies that GR paths first propagate into the network core up to the nodes with “right” maximum values of  $\omega \approx \omega_c$  and then exit the core toward low- $\omega$  destinations in the periphery. By “right”  $\omega_c$  we mean a specific scaling behavior of  $\omega_c$  as a function of distance  $d$  necessary for this hierarchical path pattern to successfully adapt to increasing  $d$ . Examination of the analytic expression for  $P_{up}(\omega, d)$  shows (see Appendix F) that  $\omega_c(d)$  scales as  $\sqrt{d}$  for navigable networks with low  $\gamma$  and high  $\alpha$ , meaning that the larger the hidden distance to a destination, the deeper, i.e., higher- $\omega$ , levels in the core that GR paths go through.

We also see in Fig. 5 that both  $w_c(d)$  scaling and, consequently, the hierarchical path pattern becomes less prominent with increase of  $\gamma$  or decrease of  $\alpha$ . This latter observation explains the non-navigability of large networks with such values of  $\gamma$  and  $\alpha$  that we detected in Figs. 1-2. In particular, the percentage of successful paths decreases with network size  $N$  for small  $\alpha$  and large  $\gamma$  in Fig. 2 because on average, hidden distances between nodes grow linearly with  $N$ , cf. Eqs. (1,4), and

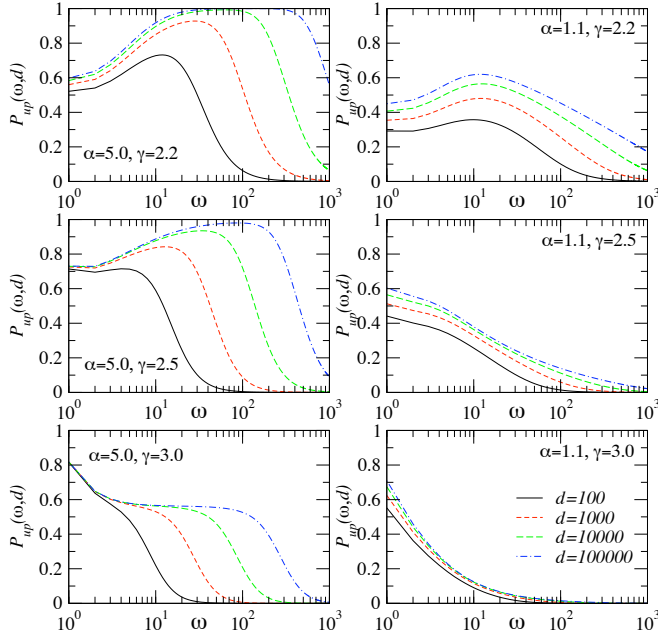


FIG. 5: **Probability**  $P_{up}(\omega, d)$  that the next hop after an  $\omega$ -labeled node at distance  $d$  from a destination has value  $\omega' \geq \omega$  and  $d' \leq d$ . The distance legend in the right-bottom plot applies to all the plots. The results are for the large-graph limit  $N \rightarrow \infty$ .

as Fig. 5 shows, the GR path structure does not properly adapt to these increasing distances. As a result, in such non-navigable networks, GR paths never reach deep in the high- $\omega$  core; even if a hidden distance to the destination is large, they stay in the low- $\omega$  periphery, where the probability of getting lost is high, cf. Fig. 4.

## B. Simulation results

In Fig. 6 we expose the structure of simulated GR paths. Fig. 6 is congruent with Fig. 5. We see that for small  $\gamma$  and large  $\alpha$  (upper left and middle left), the GR process quickly finds a way to the high- $\omega$  core, makes a few hops there, and then descends to a low- $\omega$  destination. In the opposite, non-navigable extreme of high  $\gamma$  and low  $\alpha$  (lower right plots), the GR process can almost never get to the core. Instead, it wanders in the low- $\omega$  periphery making a large number of hops there and thus increases the probability of getting lost.

## C. Discussion and explanation

We reiterate our findings to informally explain the observed phenomena.

Since we have a global view of the structure of networks in our model, we see that the optimal layout of routes in them is congruent with the network hierarchy. Indeed, an optimal path that starts in the low-degree

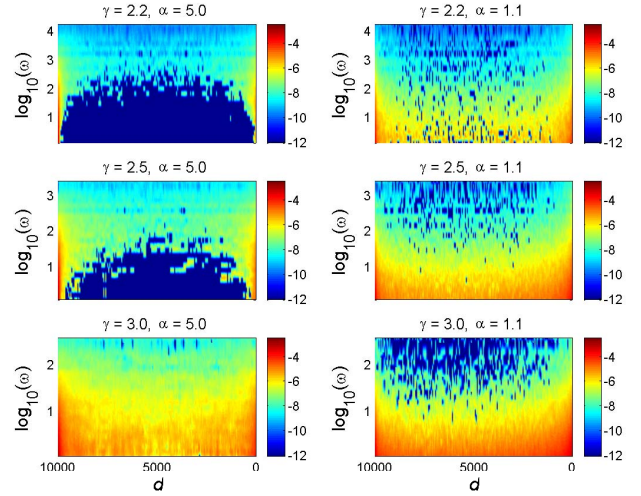


FIG. 6: **The structure of greedy-routing paths.** The color shows the logarithm of normalized densities of the number of  $\omega$ -labeled hops located at hidden distance  $d$  from a destination. All hops used to compute the densities come from random collections of successful greedy-routing paths in modeled networks with different values of  $\gamma$  and  $\alpha$ . The original number of paths is  $10^5$  in all cases, but the number of successful paths and path hop-lengths vary, cf. Figs. 2,1. All paths start at nodes  $a$  with  $\omega_a < 2$  located in the left-bottom corners of the diagrams. Values  $\omega_b$  of destinations  $b$  are not fixed, but most of them are also low, cf. Eq. (8), and located in the right-bottom corners. The initial hidden distance  $d_{ab}$  is approximately  $10^4$  and the network size  $N$  is  $10^5$  everywhere.

periphery of a network and tries to reach a remote location, also in the periphery, first penetrates into the network core. High-degree nodes there cover large hidden distances by their many connections, i.e., their characteristic distance scales are large. Just one hop in the core can thus significantly decrease the hidden distance to the destination. The path then moves out of the core to lower-degree nodes “zooming in” onto the destination.

However, our greedy navigation process does not have the full knowledge about the network structure that we do have. We do not even assume that the process is intelligent enough to know or estimate degrees of intermediate nodes, much less use this knowledge to optimize its decisions; it operates based only on hidden distances. On the other hand, both node degrees and hidden distances shape the global network structure. Therefore, the irresistible inference is that the structure of *navigable* networks must favor greedy routing in that the layout of greedy-routing paths, which ignore node degrees, must be congruent with the hierarchical “up-down” path pattern described above, which relies on node degree information.

Higher values of  $\alpha$ , i.e., stronger clustering, are desirable in this context because, all other parameters equal, they lead to larger proportions of links connecting low-degree nodes to high-degree nodes, both located at small hidden distances from each other. The larger the number

of such links, the easier it is for greedy routing to find path segments connecting the periphery and the core of a network.

Lower values of exponent  $\gamma$  correspond to more heterogeneous degree distributions and, consequently, to deeper and better-developed hierarchies of network connectivity. High  $\gamma$ -values, on the other hand, lead to imbalanced degree distributions implying, among other things, that there are just not enough high-degree nodes to cover all the hidden distance scales populated with abundant low-degree nodes.

At the same time, low  $\gamma$ -values lead to relatively larger numbers of low-degree nodes as well. The lower the degree of a node, the higher the probability for greedy routing to get lost at this node because the higher the probability that none of its neighbors lie in the needed hidden direction toward the destination. As a result, the proportion of successful paths is smaller for lower  $\gamma$ -values.

Summarizing, *navigable scale-free networks have strong clustering and power-law degree distribution exponents of  $\gamma = 2 + \epsilon$ , where  $\epsilon > 0$  is small enough to guarantee the presence of strong hierarchical structure congruent with the optimal layout of greedy-routing paths, and large enough to reduce the number of low-degree nodes at which greedy routing fails with high probability.* Most complex networks observed in reality, including the Internet, do have these properties [17].

## VI. CONCLUSION

It is a relatively unexplored question [23] whether the scale-free structure of complex networks is a cause or a consequence of their evolution toward navigable configurations, i.e., connectivity structures that are favorable for simple (quasi-)targeted information propagation strategies. This problem persists because it remains unclear what are the best and most universal ways to abstract such processes and associated attributes of nodes.

The work presented here provides a step forward by introducing a conceptually simple approach in which we abstract information propagation as a greedy-routing process that operates on top of a network and bases its routing decisions on distances within a hidden metric space lying underneath the network. These hidden distances may have different interpretations in different real networks. In the most general interpretation, they abstract similarities between nodes as in [8]. Reformulation of hidden distances as hidden variables allows us to analytically calculate the greedy-routing propagator describing the navigability of a network.

Upon studying characteristics of this propagator and

confirming them in simulations, we face a surprising coincidence: the structural properties of many complex networks observed in reality are exactly those needed to maximize their navigability. This finding evokes interesting theoretical as well as practical questions. The most interesting, but also difficult, theoretical question is whether complex networks do indeed *evolve* toward more navigable configurations. If so, it explains the remarkable coincidence that we found.

The immediate practical applications involve directed discovery of hidden metric spaces underlying concrete networks. In this paper we have shown that even the simplest possible formalization of such spaces, e.g.,  $\mathbb{S}^1$ , qualitatively yields all the remarkable effects that we have reported. Reconstruction of the explicit structure of hidden metric spaces beneath other networks, e.g., social networks, Web, etc., have straightforward implications for efficient searching strategies in such networks.

Perhaps more important is to find a hidden metric space for the global Internet, whose routing architecture bears long-standing scalability problems that are intensifying this decade [2]. A network as complex as the Internet would undoubtedly have a hidden metric space more complex than  $\mathbb{S}^1$ . But its pursuit is worthwhile, since Internet routing based on it would bring previously unimagined scaling properties, including freedom from the requirement for routers to maintain a coherent, up-to-date view of the increasingly dynamic and ever-growing global Internet topology—considered the greatest scalability challenge. Instead of incessant processing of topology updates needed to maintain this global view, routers could base their forwarding decisions only on hidden coordinates of their local neighbors. Discovery of a hidden metric space for the Internet would thus offer an exceptionally scalable routing architecture for the universal communication infrastructure of the 21st century.

In general, we hope that this work will foster further research that deepens our understanding of the fundamental laws describing relationships between structure and function of complex networks.

## Acknowledgments

We thank M. Ángeles Serrano for very useful comments and discussions, and for suggesting the idea to use  $k$ -core decomposition to visualize network hierarchies in our model. This work was supported in part by DGEs grants No. FIS2004-05923-CO2-02 and FIS2007-66485-CO2-02, Generalitat de Catalunya grant No. SGR00889, the Ramón y Cajal program of the Spanish Ministry of Science, and by NSF CNS-0434996 and CNS-0722070.

---

[1] C. B. Duke, *et al.*, ed., *Network Science* (The National Academies Press, Washington, 2006).

[2] D. Meyer, L. Zhang, and K. Fall, eds., *Report from the IAB Workshop on Routing and Addressing* (The Internet



- Architecture Board, 2007).
- [3] D. Krioukov, kc claffy, K. Fall, and A. Brady, *Comput Commun Rev* **37**, 41 (2007).
  - [4] S. Milgram, *Psychol Today* **1**, 61 (1967).
  - [5] J. M. Guiot, *Eur J of Soc Psychol* **6**, 503 (1976).
  - [6] J. Kleinberg, *Proc Int Congr Math (ICM)* (2006).
  - [7] J. Kleinberg, *Nature* **406**, 845 (2000).
  - [8] F. Menczer, *Proc Natl Acad Sci USA* **99**, 14014 (2002).
  - [9] Ö. Şimşek and D. Jensen, *Proc Int Joint Conf Artif Int (IJCAI)* (2005).
  - [10] L. A. Adamic, R. M. Lukose, A. R. Puniyani, and B. A. Huberman, *Phys Rev E* **64**, 46135 (2001).
  - [11] M. Boguñá and R. Pastor-Satorras, *Phys Rev E* **68**, 036112 (2003).
  - [12] M. A. Serrano and M. Boguñá, *Phys Rev E* **68**, 015101(R) (2003).
  - [13] Y. Y. Shi, G. A. Miller, H. Qian, and K. Bomsztyk, *Proc Natl Acad Sci USA* **103**, 11527 (2006).
  - [14] J. Matoušek, *Lectures on Discrete Geometry* (Springer, New York, 2002), chap. 15, Embedding Finite Metric Spaces into Normed Spaces.
  - [15] P. Mahadevan, D. Krioukov, M. Fomenkov, B. Huffaker, X. Dimitropoulos, kc claffy, and A. Vahdat, *Comput Commun Rev* **36**, 17 (2006).
  - [16] M. Boguñá, R. Pastor-Satorras, A. Díaz-Guilera, and A. Arenas, *Phys Rev E* **70**, 056122 (2004).
  - [17] M. E. J. Newman, *SIAM Rev* **45**, 167 (2003).
  - [18] D. J. Watts, P. S. Dodds, and M. E. J. Newman, *Science* **296**, 1302 (2002).
  - [19] M. Girvan and M. E. J. Newman, *Proc Natl Acad Sci USA* **99**, 7821 (2002).
  - [20] J. I. Alvarez-Hamelin, L. Dall'Asta, A. Barrat, and A. Vespignani, *cs.NI/0504107* (2005), URL <http://xavier.informatics.indiana.edu/lanet-vi/>.
  - [21] B. Bollobás, *Modern Graph Theory* (Springer-Verlag, New York, 1998).
  - [22] S. N. Dorogovtsev, A. V. Goltsev, and J. F. F. Mendes, *Phys Rev Lett* **96**, 040601 (2006).

[23] A. Clauset and C. Moore, *cond-mat/0309415* (2003).

## APPENDIX A: ANALYTIC VS. SIMULATION RESULTS FOR THE DEGREE DISTRIBUTION IN THE $\mathbb{S}^1$ MODEL

To check the accuracy of our analytic results for the degree distribution in the  $\mathbb{S}^1$  model, we perform numerical simulations. Fig. 7 shows excellent agreement between the degree distributions obtained from these simulations and the analytical prediction. As explained in the main text, parameter  $\alpha$  does not affect the degree distribution.

## APPENDIX B: ANALYTIC AND SIMULATION RESULTS FOR CLUSTERING IN THE $\mathbb{S}^1$ MODEL

Using the hidden-variable formalism, the clustering coefficient of a node with generic hidden variable  $h$  is given by

$$\bar{c}(h) = N^2 \int \int dh' dh'' \frac{\rho(h') \rho(h'') r(h, h') r(h', h'') r(h, h'')}{[\bar{k}(h)]^2}, \quad (\text{B1})$$

where  $\bar{k}(h)$  is the average degree of nodes with hidden variable  $h$ , that is,

$$\bar{k}(h) = N \int dh' \rho(h') r(h, h'). \quad (\text{B2})$$

Applying these equations to the  $\mathbb{S}^1$  model yields the following expression for the average clustering coefficient of  $\omega$ -labeled nodes:

$$\bar{c}(\omega) = \frac{1}{4}(\alpha - 1)^2 \int \int d\omega' d\omega'' \frac{\omega' \rho(\omega')}{\langle \omega \rangle} \frac{\omega'' \rho(\omega'')}{\langle \omega \rangle} \int_{-\infty}^{\infty} \int_{-\infty}^{\infty} \frac{dx' dx''}{(1 + |x'|)^\alpha (1 + |\omega \frac{x'}{\omega''} - \frac{x''}{\omega'}|)^\alpha (1 + |x''|)^\alpha}. \quad (\text{B3})$$

Note that the clustering is independent of the hidden position  $\theta$  of the node since  $\rho(\theta)$  is uniform and  $\mathbb{S}^1$  is isotropic.

Although Eq. (B3) is not a closed-form expression, it allows us to infer several important properties of the clustering in our model:

- There is no dependence on the size of the network, meaning that clustering stays constant in the large-graph limit  $N \rightarrow \infty$ .
- Clustering vanishes in the limit  $\alpha \rightarrow 1^+$ , indicating that, in this limit, the hidden metric structure of networks in the model is severely stressed.
- Clustering is independent of the average degree.

Fig. 8 shows simulation results for the clustering coefficient in the model. As predicted by Eq. (B3), clustering vanishes when  $\alpha$  approaches 1, whereas it converges to a constant value for large  $\alpha$ 's. In general, clustering is stronger for smaller  $\gamma$ 's.

## APPENDIX C: SELF-SIMILARITY OF THE $\mathbb{S}^1$ MODEL

The  $\mathbb{S}^1$  model produces self-similar networks. To see this fact, take a graph generated by the model and consider its subgraph composed of nodes with a value of  $\omega$  larger than a certain threshold value  $\omega_0$ . Since  $\rho(\omega)$  is

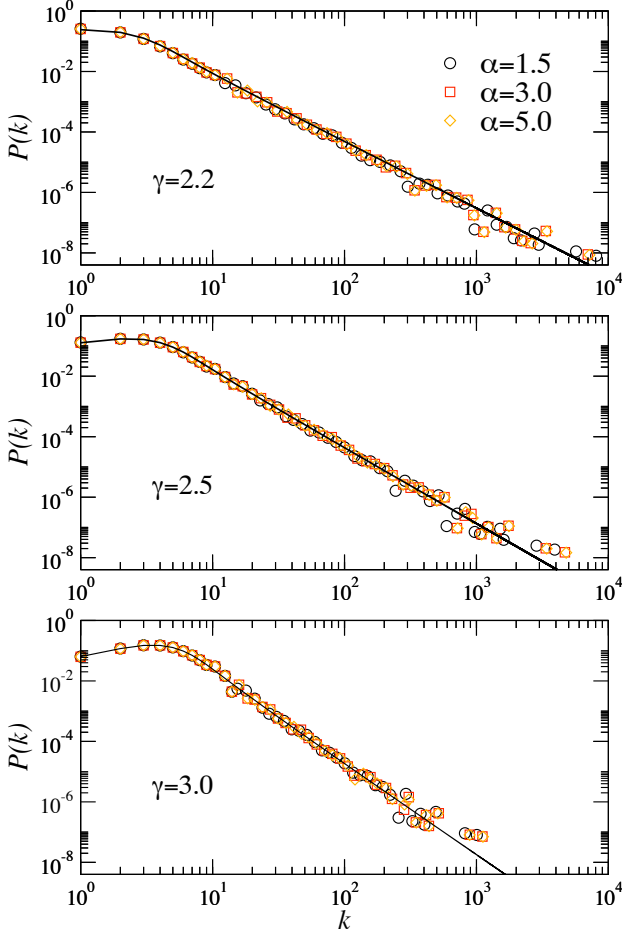


FIG. 7: Degree distributions obtained from simulation of the  $\mathbb{S}^1$  model (symbols) compared with the analytical solution (solid lines) for  $\gamma = 2.2, 2.5$ , and  $3.0$  (from top to bottom) and different values of  $\alpha$ . Simulation results are for a single network instance of size  $N = 10^5$  and  $\langle k \rangle = 6$ .

power-law distributed, the distribution of  $\omega$ 's for this sub-set is given by the same power-law function but starting at  $\omega_0$  instead of 1. Therefore, the average of  $\omega$  within the subgraph is given by  $\langle \omega(\omega_0) \rangle = \langle \omega \rangle \omega_0$ . The number of nodes with  $\omega > \omega_0$  is  $N\omega_0^{1-\gamma}$  so that the density of such nodes in the metric space is  $\delta(\omega_0) = \delta\omega_0^{1-\gamma}$ , where  $\delta$  is the density of nodes for the whole graph, which we keep fixed to 1 in the main text. Since the connection probability between nodes is the same, the described subgraph will be a replica of the whole graph after the following renormalization of the parameters:

$$\begin{aligned} \langle \omega \rangle &\longrightarrow \langle \omega \rangle \omega_0 \\ \delta &\longrightarrow \delta \omega_0^{1-\gamma} \end{aligned} \quad (C1)$$

In particular, this observation implies that the internal average degree in the subgraph is

$$\langle k(\omega_0) \rangle = \omega_0^{3-\gamma} \langle k \rangle. \quad (C2)$$

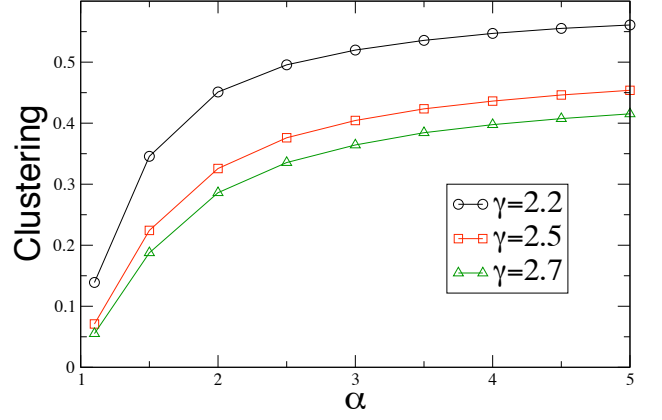


FIG. 8: Average clustering coefficient for nodes of degrees larger than 1 as a function of the parameter  $\alpha$ . The network size is  $N = 10^5$  and  $\langle k \rangle = 6$ .

The subgraph's degree distribution is given by the same analytic expression as in the main text, except that  $\langle k \rangle$  is as in Eq. (C2).

We note that the internal average degree, Eq. (C2), is a growing function of  $\omega_0$  when  $2 < \gamma < 3$ , meaning that nodes with high values of  $\omega$  (and consequently high degrees) are more tightly connected to each other than to the whole network. This effect partially explains the emergence of rich  $k$ -core structure for low  $\gamma$ 's and proves its absence when  $\gamma > 3$ . Indeed, in the latter case, high-degree nodes are with high probability not connected to each other, i.e., they become isolated in this case.

#### APPENDIX D: SMALL-WORLD PROPERTY OF THE $\mathbb{S}^1$ MODEL

The small-world property is crucial for routing. We cannot expect a routing process to follow short paths if the network does not have them. By “short” we mean, as in the existing literature, the paths with average lengths that grow polylogarithmically with the network size. While this property is usually present in random networks, it is not always the case for networks with geometric constraints.

To verify if the  $\mathbb{S}^1$  model produces small worlds, we calculate probability  $p(d, \omega|\omega')$  that an  $\omega'$ -labeled node located at  $\theta = 0$  (since  $\rho(\theta)$  is uniform and  $\mathbb{S}^1$  is isotropic, this choice of  $\theta$  does not lose generality) has a neighbor with hidden variable  $\omega$  at hidden distance  $d$  from itself. Using the hidden-variable formalism yields the answer:

$$p(d, \omega|\omega') = \frac{2\langle \omega \rangle}{\langle k \rangle \omega'} \rho(\omega) \left( 1 + \frac{d}{\kappa \omega \omega'} \right)^{-\alpha}. \quad (D1)$$

Integration over  $\omega$  gives probability  $p(d|\omega')$  that a node has a neighbor at hidden distance  $d$  from itself. For large

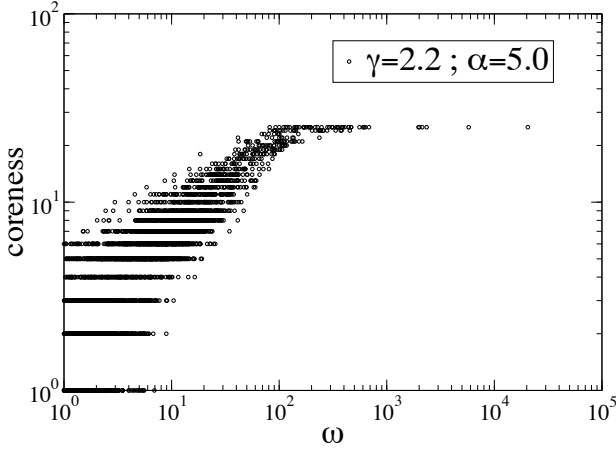


FIG. 9: Scatter plot of the coreness vs.  $\omega$  for a modeled network with  $\gamma = 2.2$ ,  $\alpha = 5.0$  and  $N = 2 \times 10^4$ .

distances  $d$ , this function behaves as

$$p(d|\omega') \sim \begin{cases} d^{-\alpha} & \text{when } \alpha < \gamma - 1, \\ d^{1-\gamma} & \text{when } \alpha > \gamma - 1. \end{cases} \quad (\text{D2})$$

The network is a small world when the average hidden distance to neighbors  $\bar{d}(\omega') = \int dp(d|\omega')dd$  diverges in the large- $N$  and, consequently, large- $d$  limit. Such divergence indicates presence of links connecting nodes located at all, including arbitrarily large, hidden distance scales. These shortcut links make short paths possible.

Average distance  $\bar{d}(\omega')$  diverges when the exponent of the asymptotic form of  $p(d|\omega')$  for large  $d$  in Eq. (D2) is smaller than 2, i.e., when either  $1 < \alpha < 2$  or  $2 < \gamma < 3$ , or both. Scale-free networks observed in reality have values of  $\gamma$  between 2 and 3, meaning that they correspond to the class of small-world networks in our model regardless of the value of  $\alpha$ .

#### APPENDIX E: CORENESS VS. $\omega$

We show coreness as a function of  $\omega$  in Fig. 9. As expected, coreness generally grows with  $\omega$ . More specifically, this growth follows a power law on average, up to the maximum coreness value, at which this growth obviously saturates.

#### APPENDIX F: THE ONE-HOP PROPAGATOR OF GREEDY ROUTING

To derive the greedy-routing propagator in this appendix, we adopt a slightly more general formalism than in the main text. Specifically, we assume that nodes live in a generic metric space  $\mathcal{H}$  and, at the same time, have intrinsic attributes unrelated to  $\mathcal{H}$ . Contrary to normed spaces or Riemannian manifolds, generic metric

spaces do not admit any coordinates, but we still use the coordinate-based notations here to simplify the exposition below, and denote by  $\mathbf{x}$  nodes' coordinates in  $\mathcal{H}$  and by  $\omega$  all their other, non-geometric attributes. In other words, hidden variables  $\mathbf{x}$  and  $\omega$  in this general formalism represent some collections of nodes' geometric and non-geometric hidden attributes, not just a pair of scalar quantities. Therefore, integrations over  $\mathbf{x}$  and  $\omega$  in what follows stand merely to denote an appropriate form of summation in each concrete case.

As in the main text, we assume that  $\mathbf{x}$  and  $\omega$  are independent random variables so that the probability density to find a node with hidden variables  $(\mathbf{x}, \omega)$  is

$$\rho(\mathbf{x}, \omega) = \delta(\mathbf{x})\rho(\omega)/N, \quad (\text{F1})$$

where  $\rho(\omega)$  is the probability density of the  $\omega$  variables and  $\delta(\mathbf{x})$  is the concentration of nodes in  $\mathcal{H}$ . The total number of nodes is

$$N = \int_{\mathcal{H}} \delta(\mathbf{x})d\mathbf{x}, \quad (\text{F2})$$

and the connection probability between two nodes is an integrable decreasing function of the hidden distance between them,

$$r(\mathbf{x}, \omega; \mathbf{x}', \omega') = r[d(\mathbf{x}, \mathbf{x}')/d_c(\omega, \omega')], \quad (\text{F3})$$

where  $d_c(\omega, \omega')$  a characteristic distance scale that depends on  $\omega$  and  $\omega'$ .

We define the one-step propagator of greedy routing as the probability  $G(\mathbf{x}', \omega'|\mathbf{x}, \omega; \mathbf{x}_t)$  that the next hop after a node with hidden variables  $(\mathbf{x}, \omega)$  is a node with hidden variables  $(\mathbf{x}', \omega')$ , given that the final destination is located at  $\mathbf{x}_t$ .

To further simplify the notations below, we label the set of variables  $(\mathbf{x}, \omega)$  as a generic hidden variable  $h$  and undo this notation change at the end of the calculations according to the following rules:

$$\begin{aligned} (\mathbf{x}, \omega) &\longrightarrow h \\ \rho(\mathbf{x}, \omega) &\longrightarrow \rho(h) \\ d\mathbf{x}d\omega &\longrightarrow dh \\ r(\mathbf{x}, \omega; \mathbf{x}', \omega') &\longrightarrow r(h, h'). \end{aligned} \quad (\text{F4})$$

We begin the propagator derivation assuming that a particular network instance has a configuration given by  $\{h, h_t, h_1, \dots, h_{N-2}\} \equiv \{h, h_t; \{h_j\}\}$  with  $j = 1, \dots, N-2$ , where  $h$  and  $h_t$  denote the hidden variables of the current hop and the destination, respectively. In this particular network configuration, the probability that the current node's next hop is a particular node  $i$  with hidden variable  $h_i$  is the probability that the current node is connected to  $i$  but disconnected to all nodes that are closer to the destination than  $i$ ,

$$\begin{aligned} \text{Prob}(i|h, h_t; \{h_j\}) &= \\ &= r(h, h_i) \prod_{j(\neq i)=1}^{N-2} [1 - r(h, h_j)]^{\Theta[d(h_i, h_t) - d(h_j, h_t)]}, \end{aligned} \quad (\text{F5})$$

where  $\Theta(\cdot)$  is the Heaviside step function. Taking the average over all possible configurations  $\{h_1, \dots, h_{i-1}, h_{i+1}, \dots, h_{N-2}\}$  excluding node  $i$ , we obtain

$$\text{Prob}(i|h, h_t, h_i) = r(h, h_i) \left(1 - \frac{1}{N-3} \bar{k}(h|h_i, h_t)\right)^{N-3}, \quad (\text{F6})$$

where

$$\bar{k}(h|h_i, h_t) = (N-3) \int_{d(h_i, h_t) < d(h', h_t)} \rho(h') r(h, h') dh' \quad (\text{F7})$$

is the average number of connections between the current node and nodes closer to the destination than node  $i$ , excluding  $i$  and  $t$ .

The probability that the next hop has hidden variable  $h'$ , regardless of its label, i.e., index  $i$ , is

$$\text{Prob}(h'|h, h_t) = \sum_{i=1}^{N-2} \rho(h') \text{Prob}(i|h, h_t; h'). \quad (\text{F8})$$

In the case of sparse networks,  $\bar{k}(h|h', h_t)$  is a finite quan-

tity. Taking the limit of large  $N$ , the above expression simplifies to

$$\text{Prob}(h'|h, h_t) = N \rho(h') r(h, h') e^{-\bar{k}(h|h', h_t)}. \quad (\text{F9})$$

Yet, this equation is not a properly normalized probability density function for the variable  $h'$  since node  $h$  can have degree zero with some probability. If we consider only nodes with degrees greater than zero, then the normalization factor is given by  $1 - e^{-\bar{k}(h)}$ . Therefore, the properly normalized propagator is finally

$$G(h'|h, h_t) = \frac{N \rho(h') r(h, h') e^{-\bar{k}(h|h', h_t)}}{1 - e^{-\bar{k}(h)}}. \quad (\text{F10})$$

We now undo the notation change and express this propagator in terms of our mixed coordinates:

$$G(\mathbf{x}', \omega' | \mathbf{x}, \omega; \mathbf{x}_t) = \frac{\delta(\mathbf{x}') \rho(\omega')}{1 - e^{-\bar{k}(\mathbf{x}, \omega)}} r \left[ \frac{d(\mathbf{x}, \mathbf{x}')}{d_c(\omega, \omega')} \right] e^{-\bar{k}(\mathbf{x}, \omega | \mathbf{x}', \omega_t)}, \quad (\text{F11})$$

with

$$\bar{k}(\mathbf{x}, \omega | \mathbf{x}', \omega_t) = \int_{d(\mathbf{x}', \mathbf{x}_t) > d(\mathbf{y}, \mathbf{x}_t)} d\mathbf{y} \int d\omega' \delta(\mathbf{y}) \rho(\omega') r \left[ \frac{d(\mathbf{x}, \mathbf{y})}{d_c(\omega, \omega')} \right]. \quad (\text{F12})$$

In the particular case of the  $\mathbb{S}^1$  model, we can express this propagator in terms of relative hidden distances instead of absolute coordinates. Namely,  $G(d', \omega' | d, \omega)$  is the probability that an  $\omega$ -labeled node at hidden distance

$d$  from the destination has as the next hop an  $\omega'$ -labeled node at hidden distance  $d'$  from the destination. After tedious calculations, the resulting expression reads:

$$G(d', \omega' | d, \omega) = \begin{cases} \frac{(\gamma-1)}{\omega'^\gamma} \left[ \frac{1}{(1+\frac{d-d'}{\kappa\omega})^\alpha} + \frac{1}{(1+\frac{d+d'}{\kappa\omega})^\alpha} \right] \exp \left\{ \frac{(1-\gamma)\kappa\omega}{\alpha-1} \left[ \mathcal{B}\left(\frac{d-d'}{\kappa\omega}, \gamma-2, 2-\alpha\right) - \mathcal{B}\left(\frac{d+d'}{\kappa\omega}, \gamma-2, 2-\alpha\right) \right] \right\} & ; d' \leq d \\ \frac{(\gamma-1)}{\omega'^\gamma} \left[ \frac{1}{(1+\frac{d'-d}{\kappa\omega})^\alpha} + \frac{1}{(1+\frac{d+d'}{\kappa\omega})^\alpha} \right] \exp \left\{ \frac{(1-\gamma)\kappa\omega}{\alpha-1} \left[ \frac{2}{\gamma-2} - \mathcal{B}\left(\frac{d'-d}{\kappa\omega}, \gamma-2, 2-\alpha\right) - \mathcal{B}\left(\frac{d+d'}{\kappa\omega}, \gamma-2, 2-\alpha\right) \right] \right\} & ; d' > d \end{cases}, \quad (\text{F13})$$

where we have defined function

$$\mathcal{B}(z, a, b) \equiv z^{-a} \int_0^z t^{a-1} (1+t)^{b-1} dt, \quad (\text{F14})$$

which is somewhat similar to the incomplete beta function  $B(z, a, b) = \int_0^z t^{a-1} (1-t)^{b-1} dt$ .

One of the informative quantities elucidating the structure of greedy-routing paths is the probability  $P_{up}(\omega, d)$  that the next hop after an  $\omega$ -labeled node at distance  $d$  from the destination has a higher value of  $\omega$ . The greedy-

routing propagator defines this probability as

$$P_{up}(\omega, d) = \int_{\omega' \geq \omega} d\omega' \int_{d' < d} dd' G(d', \omega' | d, \omega), \quad (\text{F15})$$

and we show  $P_{up}(\omega/d^{1/2}, d)$  in Fig. 10. We see that the proper scaling of  $\omega_c \sim d^{1/2}$ , where  $\omega_c$  is the critical value of  $\omega$  above which  $P_{up}(\omega, d)$  quickly drops to zero, is present only when clustering is strong. Furthermore,  $P_{up}(\omega, d)$  is an increasing function of  $\omega$  for small  $\omega$ 's only when the degree distribution exponent  $\gamma$  is close to 2.

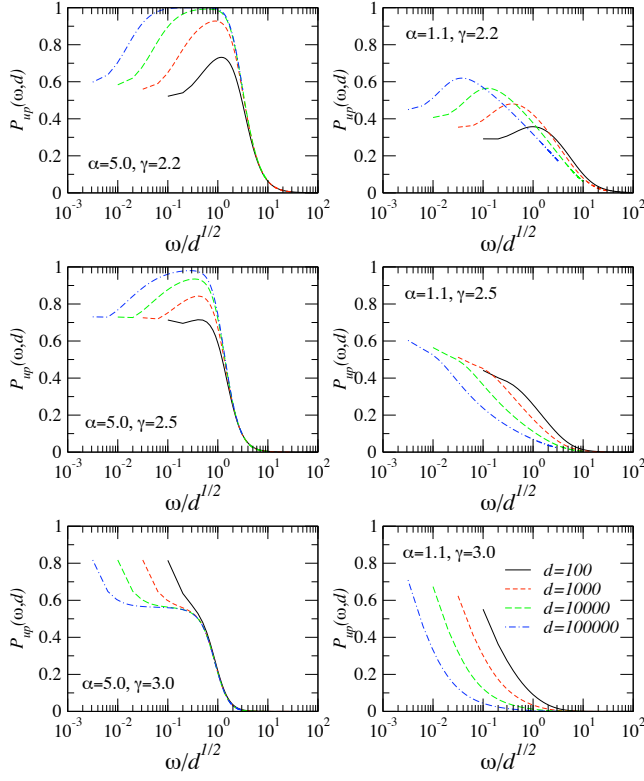


FIG. 10: Probability  $P_{up}(\omega/d^{1/2}, d)$ .

A combination of these two effects guarantees that the layout of greedy routes properly adapts to increasing distances or graph sizes, thus making networks with strong clustering and  $\gamma$ 's greater than but close to 2 navigable.